

# Linear Quadratic Regulator Design for Aircraft Longitudinal Dynamics

Linzhe (Jeremy) Wang

Fall 2023

## Abstract

The project is concentrated on the development of a control system aimed at optimizing the aircraft's response to disturbances. The goal is to ensure stability and achieve desired performance metrics. The approach involves starting with a six degrees of freedom (6DOF) nonlinear model of the aircraft. This model is linearized at trim points to facilitate the implementation of the LQR controller. The key deliverable is a comprehensive set of simulation results. These results are used to demonstrate the performance of the controller under simulated scenarios, thereby providing insights into its effectiveness and efficiency in real-world applications.

## 1 Introduction

The primary objective of this project is to design and simulate a Linear Quadratic Regulator (LQR) based controller focusing on the longitudinal dynamics of an aircraft. LQR controllers are renowned for their effectiveness in managing multivariable control problems and their unique properties. This is particularly pertinent in systems exhibiting complex dynamics, such as those encountered in aircraft control.

## 2 Problem Formulation

### 2.1 De Havilland Beaver Airfram

The aerodynamics and aircraft dynamics models are extracted from the MATLAB Aerospace Toolbox, as the project's objective emphasizes controller design. The aerodynamic data is collected using the De Havilland Beaver, a single-engine, high-wing, propeller-driven, short takeoff and landing (STOL) aircraft developed and manufactured by de Havilland Canada.



Figure 1: DHC-2 Beaver

### 2.2 Aircraft Dynamics

Consider a complete rigid-body aircraft; the moments and aerodynamic forces applied on an aircraft are caused by relative motion with respect to the air and aircraft orientation to free-stream air.

Force Equations:

$$\begin{aligned}\dot{U} &= RV - QW - g'_0 \sin \theta + \frac{F_x}{m} \\ \dot{V} &= -RV + PW + g'_0 \sin \phi \cos \theta + \frac{F_y}{m} \\ \dot{W} &= QU - PV + g'_0 \cos \phi \cos \theta + \frac{F_z}{m}\end{aligned}$$

Kinematic Equations:

$$\begin{aligned}\dot{\phi} &= P + \tan \theta (Q \sin \phi + R \cos \phi) \\ \dot{\theta} &= Q \cos \phi - R \sin \phi \\ \dot{\psi} &= \frac{Q \sin \phi}{\cos \theta} + \frac{R \cos \phi}{\cos \theta}\end{aligned}$$

Moment Equations:

$$\begin{aligned}\dot{P} &= (c_1 R + c_2 P)Q + c_3 \bar{L} + c_4 N \\ \dot{Q} &= c_5 PR - c_6 (P^2 - R^2) + c_7 M \\ \dot{R} &= (c_8 P - c_2 R)Q + c_4 \bar{L} + c_9 N\end{aligned}$$

The  $c_i$  coefficients are derived from the inertia matrix ( $J$ ) of the rigid body under the plane-of-symmetry assumption:

$$\begin{aligned}J &= \begin{bmatrix} J_x & 0 & -J_{xz} \\ 0 & J_y & 0 \\ -J_{xz} & 0 & J_z \end{bmatrix}, \quad \Gamma = J_x J_z - J_{xz}^2 \\ \Gamma c_1 &= (J_y - J_z)J_z - J_{xz}^2, \quad \Gamma c_2 = (J_x - J_y + J_z)J_{xz} \\ \Gamma c_3 &= J_z, \quad \Gamma c_4 = J_{xz} \\ c_5 &= \frac{J_z - J_x}{J_y}, \quad c_6 = \frac{J_{xz}}{J_y} \\ c_7 &= \frac{1}{J_y}, \quad \Gamma c_8 = J_x(J_x - J_y) + J_{xz}^2 \\ \Gamma c_9 &= J_x\end{aligned}$$

### 2.3 Stick Fixed Longitudinal Motion

The motion of an aircraft in free flight can be extremely complicated. However, a linearized solution can be determined by decoupling the longitudinal and lateral motions based on reasonable assumptions. For instance, in longitudinal motion, it is assumed that the aircraft only experiences small deviations from its equilibrium conditions. Furthermore, the motion of the aircraft is to be analyzed by separating it into two groups.

$$A = \begin{bmatrix} \text{Longitudinal} & \text{Longitudinal - Lateral Coupling} \\ \text{Lateral - Longitudinal Coupling} & \text{Lateral} \end{bmatrix}$$

$$B = \begin{bmatrix} \text{Longitudinal} \\ \text{Lateral} \end{bmatrix}$$

### 2.3.1 Linearized Longitudinal Motion:

$$\dot{x} = A \begin{bmatrix} \Delta u \\ \Delta w \\ \Delta q \\ \Delta \theta \end{bmatrix} + B \begin{bmatrix} \Delta \delta \\ \Delta \delta_T \end{bmatrix}$$

$$\begin{bmatrix} \Delta \dot{u} \\ \Delta \dot{w} \\ \Delta \dot{q} \\ \Delta \dot{\theta} \end{bmatrix} = \begin{bmatrix} X_u & X_w & 0 & -g \\ Z_u & Z_w & u_0 & 0 \\ M_u + M_{\dot{w}}Z_u & M_w + M_{\dot{w}}Z_w & M_q + M_{\dot{w}}u_0 & 0 \\ 0 & 0 & 1 & 0 \end{bmatrix} x + \begin{bmatrix} X_\delta & X_{\delta_T} \\ Z_\delta & Z_{\delta_T} \\ M_\delta + M_{\dot{w}}Z_\delta & M_{\delta_T} + M_{\dot{w}}Z_{\delta_T} \\ 0 & 0 \end{bmatrix} u$$

### 2.3.2 Performance Characteristic

The performance of longitudinal motion in an aircraft can be characterized by two distinct types of oscillatory motions: the short period and phugoid modes. The short period mode is a relatively fast oscillation in pitch attitude and vertical speed, involving changes in the angle of attack and pitch angle of the aircraft. In contrast, the phugoid mode is characterized by long-term, low-frequency oscillations that involve changes in altitude and speed, but with little change in attitude. This mode represents a cyclical exchange between kinetic and potential energy.

	Phugoid	Short Period
Frequency $[\frac{rad}{sec}]$	$\omega_{np} = \sqrt{\frac{-Z_u g}{u_0}}$	$\omega_{nsp} = \sqrt{\frac{Z_\alpha M_q}{u_0} - M_\alpha}$
Damping Ratio	$\zeta_p = \frac{-X_u}{2\omega_{np}}$	$\zeta_{sp} = -\frac{M_q + M_\alpha + \frac{Z_\alpha}{u_0}}{2\omega_{nsp}}$
Time to Double the Amplitude $[sec]$	$T_{2ph} = \frac{\log(2)}{-\zeta_{ph}\omega_{nph}}$	$T_{2sp} = \frac{\log(2)}{-\zeta_{sp}\omega_{nsp}}$

Table 1: Summary of Longitudinal Approximations

## 2.4 Handling Quality

Aviation regulations include a set of requirements to quantify the handling qualities of an aircraft. These requirements must be satisfied and rigorously tested prior an aircraft can receive flight certification. One notable standard, MIL-F-8785C, officially titled “Military Specification: Flying Qualities of Piloted Aircraft”, is widely used in the industry. The standard specifically defines the required flying qualities for piloted fixed-wing aircraft.

1. **Level 1:** Flying qualities clearly adequate to accomplish mission flight phase.

$$(a) \zeta_{ph} \geq 0.04, \quad 0.30 < \zeta_{sp} < 2.00$$

2. **Level 2:** Flying qualities adequate to accomplish mission flight phase with some increase in pilot workload required or degradation in mission effectiveness.

$$(a) \zeta_{ph} \geq 0.00, \quad 0.20 < \zeta_{sp} < 2.00$$

3. **Level 3:** Flying qualities adequate for airplane to be safely controlled, but excessive pilot workload is required or mission effectiveness is inadequate.

(a)  $T_{2_{ph}} \geq 55s, \quad 0.15 < \zeta_{sp}$

## 2.5 Performance without Controllers

According to Fig. 2, the De Havilland Beaver aircraft demonstrates inherent stability. However, its performance could be further enhanced by implementing an LQR (Linear Quadratic Regulator) controller. For example, the phugoid mode could be improved by increasing the damping ratio, enabling the system to meet Level 1 handling quality requirements. Additionally, an LQR controller can enhance various performance criteria, such as minimizing settling time, reducing overshoot, and achieving faster response times

	Phugoid	Short Period
Damping Ratio	$\zeta_p = 0.0354$	$\zeta_{sp} = 0.5654$

Table 2: Longitudinal Approximations for De Havilland Beaver

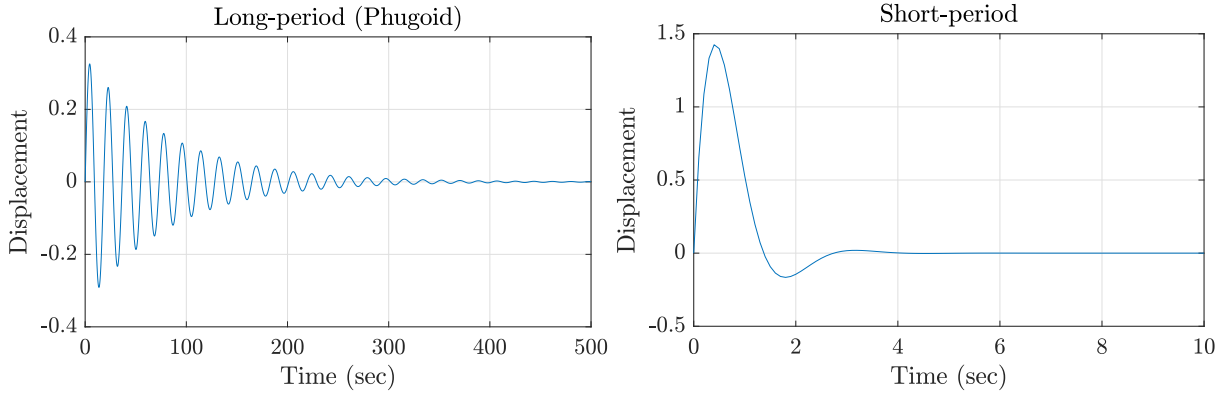


Figure 2: Flight Quality without Controllers

## 3 Methodology

### 3.1 Linearization

The 6DOF nonlinear system is linearized using the stable flight trim conditions. An input perturbation is applied to the aileron, elevator, rudder, and throttle command input ports. Output measurements are taken for states  $p$ ,  $q$ , and  $r$ .

$$x_{trim} = [U \quad V \quad W \quad \phi \quad \theta \quad \psi \quad p \quad q \quad r]^T$$

$$x_{trim} = [33.0529 \quad 0.093272 \quad 10.1004 \quad 0.0092 \quad 0.2966 \quad 0 \quad 0 \quad 0 \quad 0]^T$$

### 3.1.1 Linearized Longitudinal System

$$\dot{x} = \begin{bmatrix} 0.00745 & 0.3422 & -10.29 & -9.347 \\ -0.2811 & -0.9307 & 32.23 & -2.856 \\ 0.04963 & -0.1624 & -2.241 & 0 \\ 0 & 0 & 1 & 0 \end{bmatrix} \begin{bmatrix} U \\ W \\ q \\ \theta \end{bmatrix} + \begin{bmatrix} 0 & 0 & 0.2039 \\ 0 & -2.381 & 0 \\ 0 & -6.022 & 0 \\ 0 & 0 & 0 \end{bmatrix} \begin{bmatrix} \delta_{Aileron} \\ \delta_{Elevator} \\ \delta_{Rudder} \end{bmatrix}$$

$$y = \begin{bmatrix} 0 & 0 & 0 & 0 \\ 0 & 0 & 1 & 0 \\ 0 & 0 & 0 & 0 \end{bmatrix} \begin{bmatrix} U \\ W \\ q \\ \theta \end{bmatrix}$$

### 3.2 LQR Design

Consider the plant:

$$\dot{x} = Ax + Bu, \quad x(0) = x_0 \in \mathbb{R}^n, \quad u = Kx$$

The closed-loop system:

$$\dot{x} = (A + BK)x, \quad x(0) = x_0 \in \mathbb{R}^n$$

The objective is to design the state feedback gain  $K$  such that the closed-loop system is stable, and the pitch rate ( $q$ ) and the control effort are minimized:

$$J = \int_0^\infty (q^2 + 3u^2) dt$$

$$J = \int_0^\infty (x^T Q x + u^T R u) dt, \quad Q = Q^T \geq 0, \quad R = R^T > 0$$

Define  $Q$  and  $R$ :

$$u^T R u = 3u^2, \quad R = 3$$

$$q^2 = x^T C^T C x = x^T Q x = \begin{bmatrix} u & w & q & \theta \end{bmatrix} \begin{bmatrix} 0 & 0 & 0 & 0 \\ 0 & 0 & 0 & 0 \\ 0 & 0 & 1 & 0 \\ 0 & 0 & 0 & 0 \end{bmatrix} \begin{bmatrix} u \\ w \\ q \\ \theta \end{bmatrix} = q^2$$

Check the observability and controllability of the system, such that  $(A, B)$  is stabilizable,  $(B^T, A^T)$  is detectable, and  $(C, A)$  has no unobservable mode on  $j\mathbb{R}$ .

$$\lambda = \begin{bmatrix} -1.5698 + 2.29i & * & * & * \\ * & -1.5698 - 2.29i & * & * \\ * & * & -0.0122 + 0.3434i & * \\ * & * & * & -0.0122 - 0.3434i \end{bmatrix}$$

PBH test for observability:

$$\text{rank} \begin{bmatrix} A - \lambda(i)I \\ C \end{bmatrix} = 4 \longrightarrow \text{observable}, \quad i = (1, 1), (2, 2), (3, 3), (4, 4)$$

PBH test for controllability:

$$\text{rank} \begin{bmatrix} A^T - \lambda^{(i)} I \\ B^T \end{bmatrix} = 4 \longrightarrow \textbf{Stabilizable (dual to detectable)}, \quad i = (1, 1), (2, 2), (3, 3), (4, 4)$$

According to the Popov-Belevitch-Hautus (PBH) test, the system meets both the necessary and sufficient conditions for the LQR problem. Consequently, the optimal cost can be accurately determined by solving the associated Lyapunov equation.

$$\min_{K, X} x_0^T X x_0 \quad \text{subject to} \quad \begin{cases} X(A + BK) + (A + BK)^T X + Q + K^T R K = 0 \\ A + BK \in \mathbb{H} \end{cases}$$

The feedback gain  $K$  can be determined using the MATLAB *lqr* command:

$$\begin{aligned} -K &= \text{lqr}(A, B, C^T C, R) \\ K &= \begin{bmatrix} 0.0 & 0.0 & 0.0 & 0.0 \\ -0.0006 & -0.007 & 0.2954 & 0.1536 \\ -0.0001 & 0 & 0 & 0 \end{bmatrix} \end{aligned}$$

## 4 Results

Fig. 3 presents the closed-loop states' response and the control effort of the actuators. The plots indicate that the LQR controller ensures all state variables converge to zero, regardless of initial conditions, in accordance with closed-loop stability requirements. Furthermore, the controller is optimal in that it minimizes the cost functional  $J$ , signifying the most rapid convergence of  $x$  and  $u$  to zero. It is also worth mentioning that since the control effort is more heavily weighted in the cost functional, the amplitude of the actuators is well bounded and remains within the typical actuator duty cycle saturation.

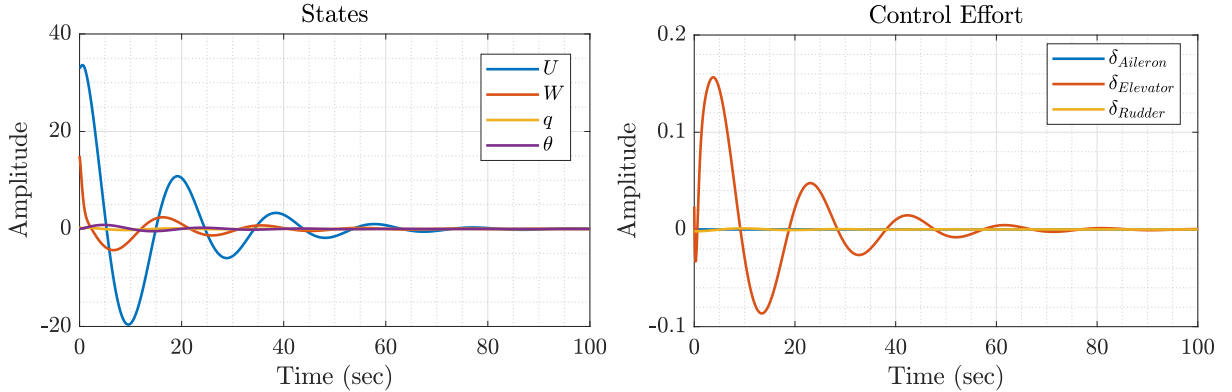


Figure 3: Closed Loop Response

Fig. 4 presents the zero and pole locations for both the original and the augmented systems. The original system's poles, being closer to the imaginary axis, indicate a high sensitivity to parameter changes. Variations in system parameters could shift these poles into the right half-plane, potentially leading to instability. In contrast, the system augmented with the LQR controller shows poles placed further from the imaginary axis, implying improved sensitivity performance. Moreover, poles located far to the left in the s-plane are

indicative of a system with effective damping and a robust response to disturbances and parameter variations. This placement suggests that the LQR-augmented system settles more quickly in response to disturbances. Therefore, the system equipped with an LQR controller demonstrates significantly enhanced performance in terms of both sensitivity and robustness compared to the original system.

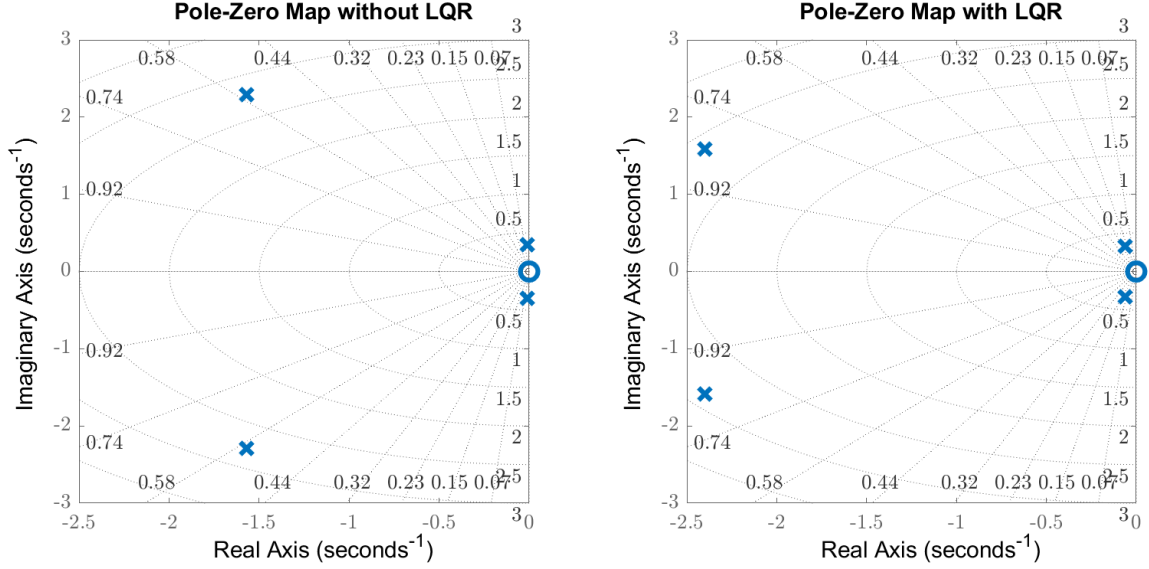


Figure 4: Pole-Zero Location

According to Fig. 5 and Tab. 3, enhancements in performance criteria such as natural frequency, damping ratio, and time to double amplitude are observed with the implementation of an LQR controller. Specifically, the damping ratio for the phugoid mode has significantly increased, resulting in improved handling quality from level 2 to level 1. Additionally, there is a marked reduction in oscillatory behavior and overshoot for both the phugoid and short-period modes, attributable to the enhanced performance of the damping ratio.

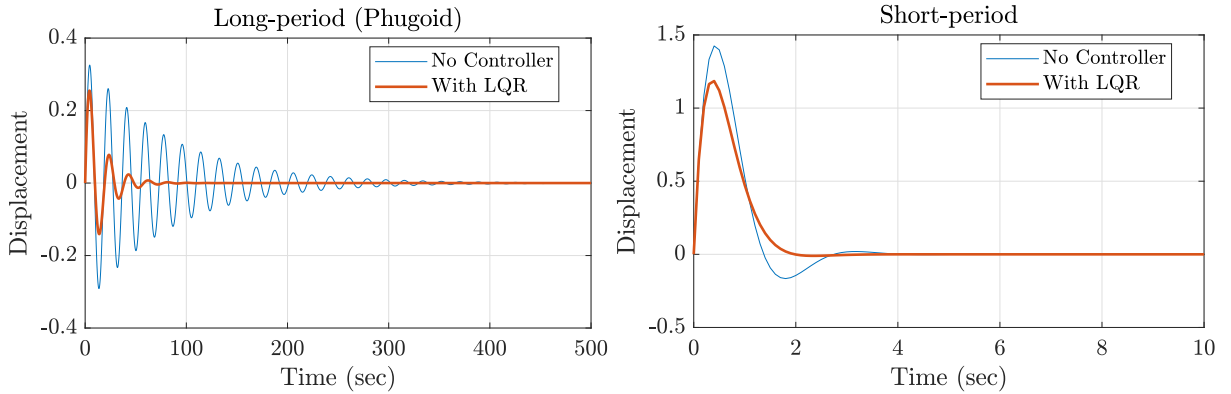


Figure 5: Flight Quality with Controllers



	Phugoid	Short Period
Frequency $[\frac{rad}{sec}]$	$\omega_{n_{ph}} = 0.3437 \rightarrow 0.3315$	$\omega_{n_{sp}} = 2.7764 \rightarrow 2.8785$
Damping Ratio	$\zeta_{ph} = 0.0354 \rightarrow 0.1859$	$\zeta_{sp} = 0.5654 \rightarrow 0.8343$
Time to Double the Amplitude $[sec]$	$T_{2_{ph}} =  -56.95  \rightarrow  -11.25 $	$T_{2_{sp}} =  -0.4416  \rightarrow  -0.2886 $

Table 3: Summary of Improvements

## 5 Conclusion

The project's objective is to design an LQR controller that optimizes the aircraft's longitudinal response to disturbances. The goal is to ensure stability and achieve desired performance metrics, such as damping ratio, natural frequency, and time to double amplitude. The approach involves starting with a six degrees of freedom (6DOF) nonlinear model of the aircraft, which is then linearized at trim points to facilitate the implementation of the LQR controller. The key deliverable is presented as a comprehensive set of simulation results, including the closed-loop system behavior, pole and zero locations of the system, and the behaviors of phugoid and short-period modes. Future work could include introducing noise into the system, designing a Kalman filter to estimate noisy states, and developing an H2 optimal controller to integrate the LQR with the Kalman filter.

## References

- [1] B. L. Stevens, F. L. Lewis, and E. N. Johnson, *Aircraft control and simulation: dynamics, controls design, and autonomous systems*. John Wiley & Sons, 2015.
- [2] R. C. Nelson *et al.*, *Flight stability and automatic control*, vol. 2. WCB/McGraw Hill New York, 1998.
- [3] MATLAB, “Flying quality analysis for 6dof de havilland beaver airframe,” tech. rep., Aerospace Blockset<sup>™</sup> and Simulink Control Design<sup>™</sup>.